

## VARIABILITY OF THE OBJECT M1–15 = SS73 6 DURING 45 YEARS

KONDRATYEVA, L.; DENISSYUK, E.; RSPAEV, F.; KRUGOV, A.

Fesenkov Astrophysical Institute, Almaty, Kazakhstan. e-mail: lu\_kondr@mail.ru

Initially the object M1–15 was included in the Catalogue of Galactic Planetary Nebulae by Perek & Kohoutek (1967), later it was classified as a Be star by Sanduleak & Stephenson (1973) and received a new designation: SS73 6. Shaw & Kaler (1989) discovered some high excitation lines of He II, 4686 Å, [OIII], 5007 Å, [NII], 6583 Å in its spectrum and suspected that this could be a symbiotic star. However later only HI, [OI] and [NII] lines were observed in the spectrum of M1–15, and no trace of a cool component was detected.

All available photometric data for this object are compiled in Table 1. Our observations were carried out in 2012 with the 1-meter Carl-Zeiss Jena reflector, located at Assy-Turgen Observatory of Fesenkov Astrophysical Institute (FAPHI). It was equipped with the CCD camera SBIG ST-7 (765 × 510, 9 $\mu$ ) and samples of *BVR* filters. HD 69901 and HD 71099 were used as standards. Increase of brightness of M1–15 by 0<sup>m</sup>.2 in all filters was registered during 1984–2012.

The main volume of spectral data was obtained with the original slit spectrograph, attached to the 0.7-m Cassegrain reflector AZT-8, located at Observatory of FAPHI. In 1971–1995 the spectrograph was equipped with the three-cascade image-tube, and the special astronomical film was used as a detector. A sample of gratings and objective lenses provided a spectral range from 3700 to 8200 Å. Since 2005 the spectrograph has been equipped with the CCD camera SBIG ST-8 (1530 × 1210, 9 $\mu$ ) with available spectral range 4000–7500 Å. The entrance slit width equals to 3'' - 4'' and 10''- 15''. Spectrograms, obtained with the broad slit are used for emission fluxes and EW determination, and those, with narrow slit for the study of emission profiles. Some spectra of M1–15 were obtained with a Shelyak eShel spectrograph and a slit spectrograph, attached to the 1-meter Carl-Zeiss Jena reflector (Tyan–Shan Observatory of FAPHI). Table 2 gives the log of observations.

All spectrograms were corrected for atmospheric extinction. There are emission lines of HI, [OI] and [NII], 6583 Å in the spectrum of M1–15. The object is observed on a background of an HII region, and an appropriate extended H $\alpha$  emission is present on our spectrograms, obtained with the maximal expose time. This line together with the sky spectrum was measured on both sides of the stellar continuum and was subtracted from the observable spectrum of the object. The absolute fluxes and equivalent widths for the H $\alpha$  and H $\beta$  are listed in Table 3. It is noticeable that the flux of H $\alpha$  increased more than twice up to 2010–2013 and then began to decrease. Behaviour of the F(H $\beta$ ) and EW values is quite similar.

Table 1: Photometric *BVR* observations of M1-15

Date	<i>B</i> mag	<i>V</i> mag	<i>R</i> mag	References
1984–1985	13.77±0.02	13.03±0.02		Shaw & Kaler, 1989
1990–1998	13.66±0.02	13.02±0.02	12.37±0.02	Vieira et al., 2003
2012	13.56±0.01	12.94±0.02	13.05±0.06	Zacharias et al., 2012
29.02.2012	13.57±0.01	12.86±0.03	12.12±0.02	FAPHI

Table 2: List of spectral observations

Date	Range (Å)	R= $\lambda/\Delta\lambda$	Telescope	Spectrograph
28.12.1973	6400-6700	7000	AZT-8 (0.7m)	Slit Spectrograph + image-tube
10.11.1991	6400-6700	7000	AZT-8 (0.7m)	Slit Spectrograph + image-tube
03.03.2005	4700-5100 6100-7100	7000 8700	AZT-8 (0.7m)	Slit Spectrograph + CCD ST-8
13.11.2010	6200-7000	13000	1-m (Assy-Turgen)	Slit Spectrograph UAGS+ CCD ST-8
05.12.2010	4700-5100	7000	AZT-8 (0.7m)	Slit Spectrograph + CCD ST-8
29.02.2012	4700-5100	7000	AZT-8 (0.7m)	Slit Spectrograph + CCD ST-8
14.02.2013	6400-6700	26000	AZT-8 (0.7m)	Slit Spectrograph + CCD ST-8
06.03.2015	6400-6700	40000	1-m (TShAO)	eShel Spectrograph +CCD STT 3200
06.03.2016	4400-5100	10000	1-m (TShAO)	Slit spectrograph +CCD ATIK 16200

This is the case when the profiles of H $\alpha$  emission lines consist of two peaks with the variable V/R ratio. The main parameters of H $\alpha$  profiles are presented in Table 4: 1 – date of observations; 2 – width of H $\alpha$  profile for  $I = 0.5 \times I_{\max}$ , 3 – distance between “blue” and “red” peaks; 4 – ratio of the maximal intensities of these peaks (V/R); 5 – heliocentric radial velocity of absorption; 6 – width of wings of the profile. All these parameters show strong variability.

Emission profiles of H $\alpha$ , obtained with resolution of 0.2– 0.5 Å/px, are presented in Fig. 1. In 1973 the profile of H $\alpha$  was broad and the ratio of maximal intensity to the level of continuum was low. Then, the profile became quite narrow and its dominance over the level of the continuum has increased. The last observations show that the profile of H $\alpha$  became the same as in the '70s. The heliocentric radial velocities of an absorption component were always close to a zero within the limits of measurement errors. We don't present data on the profiles of H $\beta$  in this paper as this line is about 20 times weaker than the H $\alpha$  line and its structure is not defined.

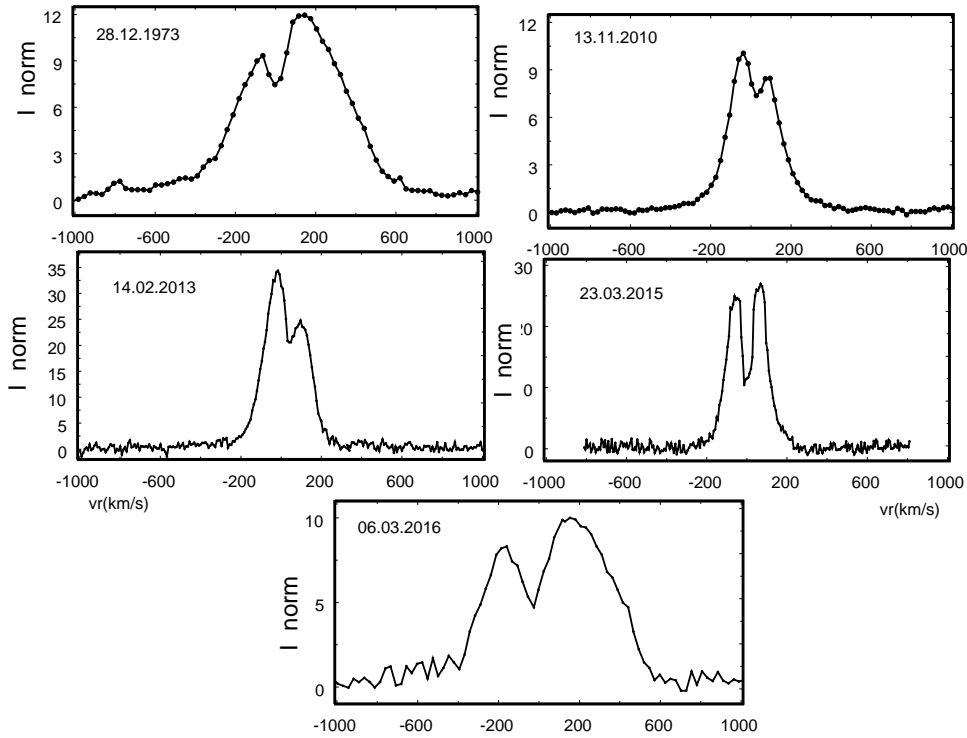
Profiles of H $\alpha$  were especially broad in 1970 and 2016. Here we consider possible mechanisms of line broadening. First of all, rotation of the circumstellar disk contributes

Table 3: Characteristics of H $\beta$  and H $\alpha$  lines

Date	HJD- 2400000	F(H $\beta$ ) $10^{-13}$	EW(H $\beta$ ) $\text{\AA}$	F(H $\alpha$ ) $10^{-12}$	EW(H $\alpha$ ) $\text{\AA}$
28.12.1973	42045.242			$2.60 \pm 0.09$	$160 \pm 10$
10.11.1991	48571.271			$3.10 \pm 0.11$	$205 \pm 12$
03.03.2005	53433.125	$2.82 \pm 0.12$	$20 \pm 1$	$5.05 \pm 0.11$	$230 \pm 10$
13.11.2010	55514.279			$6.02 \pm 0.09$	$250 \pm 10$
05.12.2010	55536.217	$2.60 \pm 0.12$	$28 \pm 2$		
29.02.2012	55987.242	$3.20 \pm 0.22$	$29 \pm 10$		
14.02.2013	56338.145			$5.42 \pm 0.04$	$265 \pm 10$
06.03.2016	57454.092	$1.65 \pm 0.11$	$20 \pm 2$	$3.44 \pm 0.12$	$210 \pm 10$

Table 4: Properties of H $\alpha$  profiles

Date	FWHM km/s	$\Delta_r$ km/s	V/R	$v_r$ km/s	Wing km/s
28.12.1973	$600 \pm 40$	$200 \pm 40$	0.78	$52 \pm 35$	$1300 \pm 60$
13.11.2010	$250 \pm 30$	$130 \pm 30$	1.12	$34 \pm 35$	$850 \pm 40$
14.02.2013	$240 \pm 15$	$100 \pm 15$	1.37	$40 \pm 10$	$650 \pm 25$
23.03.2015	$250 \pm 15$	$120 \pm 15$	0.92	$-13 \pm 10$	$600 \pm 25$
06.03.2016	$650 \pm 25$	$320 \pm 25$	0.83	$-25 \pm 23$	$1300 \pm 40$



**Figure 1.** Variation of the H $\alpha$  profiles in 1973 - 2016. X-axis shows heliocentric radial velocity (km/s), Y-axis gives the ratio  $(I_\lambda - I_{\text{cont}})/I_{\text{cont}}$

to the width of profile, but this is not enough.

It is possible that line wings are formed in the region dominated by stellar winds. There is no information about UV spectrum of M1–15, and in optical no P Cyg features were observed. Most likely this mechanism can be excluded.

Very wide H $\alpha$  emission lines may be produced by Rayleigh-Raman scattering, whereby Ly photons are converted to optical photons and fill the H $\alpha$  broad region (Arrieta & Torres-Peimbert, 2003). In the case of M1–15, the wider profiles correspond to the smaller radiation fluxes, which contradicts the results of the influence of this mechanism.

Electron scattering has been intensively studied, as the line broadening mechanism in QSOs and in WR stars. The cross section of electron scattering is independent of wavelength, thus it is expected that other intense emission lines formed in the same region as H $\alpha$  have to be similarly broad. Forbidden lines of [NII] and [OI] in the spectrum of M1–15 are seem to be sharp, but they may be formed in the more external envelope not in the central zone. Therefore, this mechanism can not be excluded.

In case of enhanced opacity, self-absorption can in principle decrease emission fluxes and cause widening of lines. The contribution of this mechanism can be significant.

Increasing of the emission fluxes may be associated with the expansion of the region of ionized gas. Accordingly, the zone of neutral gas is shifted to the outer boundaries of the circumstellar disk. With the Keplerian rotation, this leads to a decrease of rotation velocity of neutral layers and to a decrease in the distance between the profile components. Dilution of ionizing radiation will cause the opposite effect.

A period of V/R variations was not yet determined because our data points are ranged rather randomly. If the V/R ratios vary cyclically, that effect may arise from rotation of a circumstellar disk with a non-axisymmetric density distribution. Otherwise, changes of V/R ratio may be caused by incidental density perturbations of the disk.

**Acknowledgements:** This work has been supported by the Ministry of Education and Science of Republic Kazakhstan - Project No 0073/TFP “Astrophysical studies of stellar and planetary systems”.

#### References:

- Arrieta, A., Torres-Peimbert, S., 2003, *ApJS*, **147**, 97 DOI  
Pereira, C., Franco, C., de Araujo, F., 2003, *A&A*, **397**, 927 DOI  
Sanduleak, N., Stephenson, C., 1973, *ApJ*, **185**, 899 DOI  
Shao, R., Kaler, J., 1989, *ApJS*, **69**, 495 DOI  
Vieira, S., Corradi, S., de Alencar, D., et al., 2003, *AJ*, **126**, 2971 DOI  
Zacharias, N. Finch, C., Girard, T., et al., 2012, VizieR On-line Data Catalog: I/322A